Temporal diversity on DS-CDMA communication systems for blind array signal processing

Daniel Pérez Palomar and Miguel Angel Lagunas

Department of Signal Theory and Communications
Universitat Politècnica de Catalunya
c/ Jordi Girona, 1-3, Mòdul D5, Campus Nord UPC
08034 Barcelona (SPAIN)

Abstract

Many array signal processing algorithms have been developed to reject interfering signals and, therefore, increase the quality of the communication link. Some of them are reference-based and some others are blind, i.e., without any side information. A specific type of deterministic blind beamforming algorithms, named self-reference, is treated in the paper. Self-reference beamforming is suitable for signals presenting a diversity or a redundancy structure. This type of signals exhibit the property of exact self-prediction that allows the definition of an error signal to be minimized.

In the present paper, the time diversity present in the well-known DS-CDMA communication system is analyzed. Blind approaches are derived from the property of exact self-prediction arising from the implicit time redundancy encountered in the spreading codes, and from the explicit time redundancy that can also be induced by the transmitter. The proposed methods do not require, unlike most blind subspace-based techniques, any kind of spectral matrix decomposition, with the consequent reduction of complexity and computational burden. The presented methods were tested via simulations and compared to the classical Time Reference Beamformer (TRB) in terms of SINR and BER, showing a performance slightly better than a TRB scheme with 10% of the bits as a training sequence.

Key words: Blind, self-reference, self-prediction, beamforming, array signal processing, subspace methods, DS-CDMA, spread spectrum, diversity, redundancy, PN.

⋆ This work was partially supported by the European Comission under Project IST-1999-11729 METRA; the Spanish Government (CICYT) TIC98-0703, TIC99-0849; and the Catalan Government (CIRIT) 1998SGR 00081, 1999FI 00588.
[1] E-mails: {daniel,miguel}@gps.tsc.upc.es

1 Introduction

Array signal processing techniques use spatial diversity as a means to reject interfering signals according to their bearing angles or spatial signatures. The design of the beamformer requires some information about the signal of interest. The classical beamforming methods are reference-based; depending on the character of this information they can be classified into Time Reference Beamformer (TRB) and Spatial Reference Beamformer (SRB). TRB requires a training sequence to be transmitted, which implies a loss of spectral efficiency and channel bandwidth utilization but yields robust methods. SRB requires knowledge of the direction of arrival (DOA) of the signal of interest, knowledge of the array geometry, and strict array calibration.

An alternative to requiring either a spatial or a time reference are blind beamforming algorithms. They are based on deterministic or statistical properties that the desired signal is known to possess; for man-made signals, these properties are in general well-known. Blind spatial processing techniques can be applied to existing systems without the need of any modification of the transmitter, e.g. the uplink channel of a cellular communication system. Blind methods based only on signal properties do not make any a priori assumption regarding the array geometry, which makes them robust algorithms to spatial signature mismatch. It is important to note that each particular transmission scheme presents a different signal structure and, therefore, requires a specific blind method properly tailored to it.

Some of the most representative deterministic blind methods are based on properties such as the Constant Modulus [1,2], or the Finite Alphabet [3], which is exploited by decision-directed approaches. Statistical blind methods are, in general, based on high order statistics (HOS) [4,5], and cyclostationary properties [6]; they have worse convergence properties than the deterministic ones.

In this paper, a particular subset of deterministic blind algorithms, termed self-reference methods, is considered. These methods rely on the existence of a redundancy structure within the signal of interest, i.e., a diversity scheme [7]. Whenever this redundancy is present, it can be directly related to the property of exact prediction, by which we can consider that the signal possesses embedded self-references. The idea of introducing diversity or redundancy is an old one; we just have to think of channel coding consisting of the introduction of redundancy (in the Galois field) to improve the final quality of the communication link. Introduction of redundancy in the linear complex field has also been used in some areas such as equalization [8,9], beamforming in frequency diversity schemes [10,11], and beamforming in Direct Sequence Code Division Multiple Access (DS-CDMA) [12,13]. See [7] for a general diversity-based beamforming description applied to Spread Spectrum (SS) communication systems.

Diversity-based beamforming combines the use of spatial diversity at the receiver with other types of diversity inherent to the signal of interest or to the channel. In the present paper, the temporal diversity of a DS-CDMA signal is used to perform optimum single-user blind beamforming in the sense of maximum Signal to Interference-plus-Noise Ratio (SINR). Two different schemes are studied: first, the inherent temporal diversity of a DS-CDMA signal is used as a self-reference signal in a blind manner and, second, a novel alternative scheme that introduces a fixed redundancy in the PN sequence in transmission is considered as a means to allow beamforming in reception without PN synchronization. The proposed methods do not require, unlike most blind subspace-based techniques, any kind of spectral matrix decomposition, with the consequent reduction of complexity and computational burden.

In Section 2, the general concept of diversity or redundancy is introduced and effective ways of using it for blind array signal processing are described. Sections 3 and 4 are devoted to analyzing the temporal diversity of a DS-CDMA communication system, both the implicit (regular PN sequence) and the explicit one (redundancy explicitly introduced). In Section 5, a subspace perspective of the redundancy-based methods is given. Section 6 deals with the design of the redundancy structure when explicitly introduced, so that the PN correlation properties are not destroyed and the users do not interfere with each other. Comments and extensions of the presented techniques are given in Section 7. In Section 8, the proposed methods are tested and compared with the classical TRB in terms of bit error rate (BER) and SINR. Finally, in Section 9, we summarize the main results of the paper.

2 The general concept of Diversity

Diversity refers to the existence of replicas of the same signal, providing the signal structure with an inherent redundancy. It is a concept closely related to multiplexing, which implies the combination of different signals from different users. Both terms can be lumped together into the more general idea of combining a number of signals—either the same signal or different signals from different users—in such a way that it is always possible to separate them out again. The combination of these sets of signals or diversity branches can be done in any of the support axes, namely: time, frequency, code and space [2].

In the context of multiplexing, these four axes give rise to four types of mul-

[2] Other support axes can also be considered, such as the polarization axis.

tiplexing techniques: *i*) *Time Division Multiple Access* (TDMA), the use of non-overlapping time slots for each user, *ii*) *Frequency Division Multiple Access* (FDMA), the use of non-overlapping frequency bands for each user, *iii*) *Code Division Multiple Access* (CDMA), the employment of a different code (linearly independent and quasi-orthogonal) for each user, overlapping over the time and frequency axes, and *iv*) *Space Division Multiple Access* (SDMA), where each user presents a different spatial signature.

In the same way, four kinds of diversity can be identified: *i*) *Time Diversity*, simple repetition of the signal in different non-overlapping time slots, e.g., a single user in *Direct Sequence* CDMA (DS-CDMA) [12] or the spontaneous phenomenon of multipath in frequency selective channels (efficiently utilized by the RAKE receiver [14] and also commonly referred to as frequency diversity or path diversity), *ii*) *Frequency Diversity*, transmission of the same signal in different non-overlapping frequency bands, e.g., Frequency Diversity Spread Spectrum (FDSS) [15] and fast Frequency Hopping (FH), *iii*) *Code Diversity*, transmitting the same signal with different codes or spreading signatures (overlapping over the time and frequency axes) [16], and *iv*) *Space Diversity*, caused by the multipath phenomenon since each ray comes from a different direction of arrival (this diversity can only be exploited at the receiver by the use of antenna arrays). Other forms of diversity that have also been explored for exploitation in communications systems are polarization diversity [17] and Doppler diversity [18]. Clearly, when diversity is used for transmission of a signal, the available power has to be distributed over the replicas.

Self-replicas can be seen as embedded self-reference signals that give rise to the important property of self-prediction, i.e., some replicas of the signal can be predicted using other replicas [10]. This property has also been called the self-coherence property, giving name to the Self-COherence REstoral algorithm (SCORE) [6], which was applied to cyclostationary signals.

To derive the basic methodology, we assume that there are two available signals—two diversity branches—$y_1(t)$ and $y_2(t)$, composed of a correlated desired component, $d(t)$, and of uncorrelated noise terms, $n_1(t)$ and $n_2(t)$:

$$y_1(t) = \alpha d(t) + n_1(t) \tag{1}$$

$$y_2(t) = d(t) + n_2(t), \tag{2}$$

where α is the normalized cross-correlation coefficient between $y_1(t)$ and $y_2(t)$.

These two signals clearly exhibit the key feature of *exact self-prediction.* This means that it is possible to predict the desired component of one signal using the other one. In other words, we can define a prediction error that will be composed only of interference and noise. Therefore, this prediction error can be used as the objective function to minimize:

$$e(t) = y_1(t) - \alpha y_2(t), \tag{3}$$

where α is, in general, a complex constant. In the following, $\alpha = 1$ is assumed (case of equal-power and phase-aligned replicas) for simplicity of presentation.

In terms of communications, predictability can be viewed as redundancy introduced in the transmitted signal. In fact, channel coding can be viewed as a procedure to introduce non-linear [3] predictability among the coded symbols from the information symbols.

In the context of array signal processing, each signal, $y_1(t)$ and $y_2(t)$, represents the beamforming output from snapshots corresponding to two different branches $\mathbf{x}_1(t), \mathbf{x}_2(t) \in \mathbb{C}^{Q\times 1}$(with Q the number of antenna elements in the array):

$$\mathbf{x}_1(t) = \mathbf{x}_d(t) + \mathbf{n}_1(t) \tag{4}$$
$$\mathbf{x}_2(t) = \mathbf{x}_d(t) + \mathbf{n}_2(t), \tag{5}$$

where $\mathbf{x}_d(t)$ represents the common desired component of the received snapshots, and $\mathbf{n}_1(t)$ and $\mathbf{n}_2(t)$ correspond to the uncorrelated interference-plus-noise terms.

After beamforming of each branch with its corresponding beamvector, the output signals can be expressed as

$$y_1(t) = \mathbf{w}_1^H \mathbf{x}_1(t) = d(t) + n_1(t) \tag{6}$$
$$y_2(t) = \mathbf{w}_2^H \mathbf{x}_2(t) = d(t) + n_2(t), \tag{7}$$

where $\mathbf{w}_i$ is the beamvector of branch i.

The desired and interference-plus-noise average power values can be defined as

$$P_d \triangleq E\{|d(t)|^2\} = \frac{1}{2}\left[E\left\{y_1(t)y_2^*(t)\right\} + E\left\{y_2(t)y_1^*(t)\right\}\right] \tag{8}$$
$$P_{in} \triangleq \frac{1}{2}\left[E\left\{|n_1(t)|^2\right\} + E\left\{|n_2(t)|^2\right\}\right] = \frac{1}{2}E\left\{|e(t)|^2\right\}, \tag{9}$$

where uncorrelation among the desired and noise terms has been assumed. The derivation of the beamvectors will be based on the maximization of the SINR:

$$\text{SINR} \triangleq \frac{P_d}{P_{in}} = \frac{\mathbf{w}_1^H E\left\{\mathbf{x}_1(t)\mathbf{x}_2^H(t)\right\}\mathbf{w}_2 + \mathbf{w}_2^H E\left\{\mathbf{x}_2(t)\mathbf{x}_1^H(t)\right\}\mathbf{w}_1}{\mathbf{w}_1^H E\left\{\mathbf{n}_1(t)\mathbf{n}_1^H(t)\right\}\mathbf{w}_1 + \mathbf{w}_2^H E\left\{\mathbf{n}_2(t)\mathbf{n}_2^H(t)\right\}\mathbf{w}_2}. \tag{10}$$

[3] It is linear in the Galois field, but nonlinear in the complex field.

In some situations, we can assume the existence of a unique optimum beamvector $\mathbf{w}$ for all the branches (see [6,10,11] for the general case of different beamvectors), and the following definitions can be used:

$$\mathbf{R}_d \triangleq E\left\{\mathbf{x}_1(t)\mathbf{x}_2^H(t)\right\} + E\left\{\mathbf{x}_2(t)\mathbf{x}_1^H(t)\right\} \tag{11}$$
$$\mathbf{R}_{in} \triangleq E\left\{\left(\mathbf{x}_1(t) - \mathbf{x}_2(t)\right)\left(\mathbf{x}_1(t) - \mathbf{x}_2(t)\right)^H\right\}. \tag{12}$$

The SINR can be then compactly expressed as

$$\mathrm{SINR} = \frac{\mathbf{w}^H\mathbf{R}_d\mathbf{w}}{\mathbf{w}^H\mathbf{R}_{in}\mathbf{w}}. \tag{13}$$

It is very important to remark that the solution to the maximization of the SINR is identical to the solution that maximizes the following Rayleigh quotients:

$$\frac{\mathbf{w}^H\mathbf{R}_x\mathbf{w}}{\mathbf{w}^H\mathbf{R}_{in}\mathbf{w}} \quad \text{and} \quad \frac{\mathbf{w}^H\mathbf{R}_d\mathbf{w}}{\mathbf{w}^H\mathbf{R}_x\mathbf{w}}, \tag{14}$$

where the global covariance matrix is $\mathbf{R}_x = \mathbf{R}_d + \mathbf{R}_{in}$.

In practice, $\mathbf{R}_x$ can always be easily estimated from the received snapshots. Therefore, the difficulty will come from the estimation of either $\mathbf{R}_d$ or $\mathbf{R}_{in}$, which can be performed in a blind manner using the exact prediction property. The following sections are devoted to their estimation.

Once the matrices $\mathbf{R}_x$ and $\mathbf{R}_d/\mathbf{R}_{in}$ have been estimated, the spatial filter can be easily derived. The beamvector that maximizes the generic Rayleigh quotient corresponding to the matrix pencil $(\mathbf{A}, \mathbf{B})$ is given by the generalized eigenvector $\mathbf{w}$ corresponding to the maximum generalized eigenvalue:

$$\mathbf{A}\mathbf{w} = \lambda_{\max}\mathbf{B}\mathbf{w}. \tag{15}$$

The computationally expensive calculation of the generalized eigenvector of (15) can be efficiently implemented using a gradient-type adaptive algorithm maximizing the Lagrangian of the constrained maximization problem with respect to $\mathbf{w}^*$ [19,20]:

$$\frac{\partial \mathcal{L}}{\partial \mathbf{w}^*} = \mathbf{A}\mathbf{w} - \lambda\mathbf{B}\mathbf{w}, \tag{16}$$

or an iterative approach such as the *Power Iteration Method* [21], which allows the computation of the eigenvector corresponding to the eigenvalue with greatest magnitude (provided that $\mathbf{B}$ is non-singular, which is true for both $\mathbf{R}_{in}$ and $\mathbf{R}_x$):

$$\left(\mathbf{B}^{-1}\mathbf{A}\right)\mathbf{w} = \lambda_{\max}\mathbf{w}. \tag{17}$$

The *Power Iteration Method* presents a really fast convergence and, therefore, will be used in the numerical simulations of this paper. Note that as $\mathbf{B}$ is being updated with new received snapshots, $\mathbf{B}^{-1}$ can be efficiently computed using the matrix inversion lemma.

3 Implicit time-diversity in DS-CDMA

DS-CDMA is a well-known means to overlay different users overlapping both in time and frequency. It consists of multiplying each symbol by a chip sequence or spreading code with a higher signaling rate [22] (we only consider the case of long codes, i.e., time varying codes from symbol to symbol). This has the effect of spreading the signal on the frequency domain, which is a way of combating frequency-selective fading channels and narrowband interference signals. This signaling scheme exhibits the property of exact block prediction in time domain, i.e., each chip can be predicted from any other within a block—assuming knowledge of the spreading code and PN synchronization [12]. It is, therefore, a time-diversity or time-redundant scheme.

We define a block-snapshot model composed of the snapshots corresponding to all the chips within a symbol after chip pulse matched filtering and sampling at the chip rate (an oversampled signal can also be accommodated in the signal model with some modifications), $\mathbf{X}(n) \in \mathbb{C}^{Q\times \mathrm{SF}}$, as

$$\begin{aligned}\mathbf{X}(n) &= \begin{bmatrix}\mathbf{x}_1(n) & \cdots & \mathbf{x}_{\mathrm{SF}}(n)\end{bmatrix} \\ &= s_d(n)\mathbf{a}_d\mathbf{c}_d^H(n) + \sum_{i=1}^{N_I}\mathbf{a}_i\mathbf{s}_i^H(n) + \mathbf{W}(n)\end{aligned} \quad (18)$$

where n is the symbol index, $\mathbf{x}_i(n)$ the ith chip of symbol n, SF the spreading factor, $s_d(n)$ the symbol transmitted by the desired user at discrete-time n, $\mathbf{a}_d$ the steering vector of the desired user, $\mathbf{c}_d^H(n)$ the corresponding time-varying binary *i.i.d.* spreading code of the desired user along the symbol period, N_I is the number of interfering signals (other users), $\mathbf{a}_i$ the steering vector of the ith interfering user, $\mathbf{s}_i^H(n)$ the corresponding time-varying binary *i.i.d.* unsynchronized ith temporal signal along the symbol period, and $\mathbf{W}(n) \in \mathbb{C}^{Q\times \mathrm{SF}}$ is the block snapshot corresponding to the thermal noise—assumed temporally and spatially white. Note that the signal model of (18) assumes no inter-symbol interference (ISI), i.e., a channel with a low temporal dispersion. Nevertheless, for highly dispersive channels, a simple extension can be utilized as will be explained later on.

In a real situation, the signals are stationary along a symbol period, therefore, a single beamvector suffices. Assuming PN synchronization with the desired user, the block snapshot can be despread or *polarized* so that the time signal of the user of interest appears fully correlated along the symbol period:

$$\begin{aligned}\tilde{\mathbf{X}}(n) &= \mathbf{X}(n) \cdot \mathrm{diag}(\mathbf{c}_d(n)) \\ &= s_d(n)\mathbf{a}_d\mathbf{1}^H + \sum_{i=1}^{N_I} \mathbf{a}_i\tilde{\mathbf{s}}_i^H(n) + \tilde{\mathbf{W}}(n)\end{aligned} \tag{19}$$

where $\tilde{\mathbf{X}}(n)$ is the despread block snapshot, $\tilde{\mathbf{s}}_i^H(n)$ is a binary *i.i.d.* temporal sequence corresponding to user ith, and $\mathrm{diag}(\mathbf{v})$ denotes a square diagonal matrix containing $\mathbf{v}$ along its main diagonal. Note that in $\tilde{\mathbf{X}}(n)$ the desired user time signature is completely correlated, represented by $\mathbf{1}^H \in \mathbb{C}^{1\times \mathrm{SF}}$, whereas the interfering signals still appear as random time-varying binary *i.i.d.* signals $\tilde{\mathbf{s}}_i^H(n)$. This process of selective *polarization* or despreading is illustrated in Figure 1.

Once the desired signal is fully correlated among the diversity branches, it is easy to verify:

$$E\left\{\tilde{\mathbf{x}}_i(n)\tilde{\mathbf{x}}_j^H(n)\right\} = p_s\mathbf{a}_d\mathbf{a}_d^H \qquad \text{for} \quad i \neq j \tag{20}$$

$$\frac{1}{2}E\left\{\left(\tilde{\mathbf{x}}_i(n) - \tilde{\mathbf{x}}_j(n)\right)\left(\tilde{\mathbf{x}}_i(n) - \tilde{\mathbf{x}}_j(n)\right)^H\right\} = \sum_{i=1}^{N_i} p_i\mathbf{a}_i\mathbf{a}_i^H + \sigma_n^2\mathbf{I} \qquad \text{for} \quad i \neq j, \tag{21}$$

where $\tilde{\mathbf{x}}_i(n)$ is the ith column of $\tilde{\mathbf{X}}(n)$, $p_s = E\{|s_d(n)|^2\}$, and p_i is defined similarly for the ith interfering user. The derivation of $\mathbf{R}_d$ and $\mathbf{R}_{in}$ is then straightforward by means of equations (11) and (12) respectively. Since a number of SF diversity branches are available, the expression of the covariance matrices can be expressed as [4]

$$\mathbf{R}_d = \frac{1}{\mathrm{SF}(\mathrm{SF}-1)} \sum_{i=1}^{\mathrm{SF}} \sum_{\substack{j=1 \\ j\neq i}}^{\mathrm{SF}} E\left\{ \tilde{\mathbf{x}}_i(n) \tilde{\mathbf{x}}_j^H(n) \right\}$$

$$= \frac{1}{\mathrm{SF}(\mathrm{SF}-1)} E\left\{ \tilde{\mathbf{X}}(n) \left(\mathbf{1}_{\mathrm{SF}} - \mathbf{I}_{\mathrm{SF}} \right) \tilde{\mathbf{X}}^H(n) \right\} \tag{22}$$

$$\mathbf{R}_{in} = \frac{1}{2\mathrm{SF}(\mathrm{SF}-1)} \sum_{i=1}^{\mathrm{SF}} \sum_{\substack{j=1 \\ j\neq i}}^{\mathrm{SF}} E\left\{ \left(\tilde{\mathbf{x}}_i(n) - \tilde{\mathbf{x}}_j(n) \right) \left(\tilde{\mathbf{x}}_i(n) - \tilde{\mathbf{x}}_j(n) \right)^H \right\}$$

$$= \frac{1}{\mathrm{SF}(\mathrm{SF}-1)} E\left\{ \tilde{\mathbf{X}}(n) \left(\mathrm{SF} \cdot \mathbf{I}_{\mathrm{SF}} - \mathbf{1}_{\mathrm{SF}} \right) \tilde{\mathbf{X}}^H(n) \right\} \tag{23}$$

$$\mathbf{R}_x = \frac{1}{\mathrm{SF}} \sum_{i=1}^{\mathrm{SF}} E\left\{ \tilde{\mathbf{x}}_i(n) \tilde{\mathbf{x}}_i^H(n) \right\} = \frac{1}{\mathrm{SF}} E\left\{ \tilde{\mathbf{X}}(n) \tilde{\mathbf{X}}^H(n) \right\} \tag{24}$$

where $\mathbf{I}_{\mathrm{SF}} \in \mathbb{C}^{\mathrm{SF}\times\mathrm{SF}}$ and $\mathbf{1}_{\mathrm{SF}} \in \mathbb{C}^{\mathrm{SF}\times\mathrm{SF}}$ are the identity matrix and the all-one matrix respectively. The final expression for the estimation of $\mathbf{R}_d$, eq.(22), which has been derived from a viewpoint of chip-level cross-correlation properties using the key feature of exact prediction, is equivalent to that found by Suard *et al.* in [23] from a matched filtering perspective. In [24], a blind beamforming method is derived for the case of DS-CDMA using fixed codes (also known as deterministic codes or short codes).

4 Explicit fixed time-diversity in DS-CDMA

The main drawback of using directly the implicit redundancy of a DS-CDMA system is the requirement of PN synchronization. This means that the beamforming stage will not be able to work until the PN synchronization has been accomplished. For adverse environments with many interfering signals and possibly a significant near-far effect, this can be a really hard task to achieve. It would be interesting, therefore, to have a fixed structure over the time-varying spreading codes, so that the beamforming stage could start functioning before having global PN synchronization. This way, the beamforming would help the PN synchronization stage by spatially nulling out the interfering signals while achieving the required block timing to work properly (see [8] for a description of a possible synchronization approach based on the idea of designing beamvectors for different delay hypotheses in parallel and then selecting the one yielding maximum SINR as the synchronized one).

[4] Note that in a realistic implementation, the covariance matrices are estimated by approximating the expectation operator, $E\{\cdot\}$, with an average over blocks. In such a case, the estimation benefits from using all possible cross-correlation combinations instead of just two.

The block snapshot signal model to be used in this case is the same as (18), where the modified spreading code to be used—redundant PN (RPN)—has a fixed redundancy structure introduced by a linear transformation on a frame basis. This can be represented by the redundancy matrix $\mathbf{G}$ (see [8,9] for other examples of induced redundancy):

$$\tilde{\mathbf{c}}(n) = \mathbf{G}\mathbf{c}(n), \tag{25}$$

where matrix $\mathbf{G} \in \mathbb{C}^{\text{SF}\times(\text{SF-R})}$ introduces R redundant chips on the original PN segment $\mathbf{c}(n) \in \mathbb{C}^{(\text{SF}-R)\times 1}$ to be converted into the RPN segment $\tilde{\mathbf{c}}(n) \in \mathbb{C}^{\text{SF}\times 1}$. The structure introduced with the redundancy matrix $\mathbf{G}$ can be regarded as a password to the filtering process, meaning that only the signal having a pre-selected block prediction structure is considered as desired signal, rejecting any other signal with a different redundancy structure.

In this paper, since we require the finite alphabet or constellation of the signaling scheme not to be altered, we will constrain $\mathbf{G}$ to simply repeat some chips of the original spreading code—with a possible change of sign—plus a permutation (see Figure 2 (c), where the matrices used have been defined as in Figure 3). Therefore, although $\tilde{\mathbf{c}}(n)$ is time-varying, it exhibits a fixed structure that allows the employment of the exact-prediction property requiring only block timing.

The receiver will extract the set of repeated chips and will group them into two block-snapshots corresponding to two branches of temporal diversity:

$$\mathbf{X}_1(n) = \mathbf{X}(n)\mathbf{H}_1 \tag{26}$$

$$\mathbf{X}_2(n) = \mathbf{X}(n)\mathbf{H}_2 \tag{27}$$

where $\mathbf{H}_i \in \mathbb{C}^{\text{SF}\times R}$ extracts R snapshots corresponding to the ith branch into $\mathbf{X}_i \in \mathbb{C}^{Q\times R}$ (see the example in Figure 3).

By denoting:

$$\mathbf{y}_1^H(n) = \mathbf{w}^H\mathbf{X}_1(n) \tag{28}$$

$$\mathbf{y}_2^H(n) = \mathbf{w}^H\mathbf{X}_2(n), \tag{29}$$

we can define the prediction error vector as $\mathbf{e}(n) = \mathbf{y}_1(n) - \mathbf{y}_2(n)$ or, equivalently:

$$\begin{aligned} \mathbf{e}^H(n) &= \mathbf{w}^H\left(\mathbf{X}_1(n) - \mathbf{X}_2(n)\right) \\ &= \mathbf{w}^H\mathbf{X}(n)\mathbf{H}, \end{aligned} \tag{30}$$

where matrix $\mathbf{H} = (\mathbf{H}_1 - \mathbf{H}_2)$ is reminiscent of the check-parity matrix in coding theory (since it gives a zero error vector in a noisefree case). Therefore, the interference-plus-noise and global covariance matrices are given by:

$$\mathbf{R}_{in} = \frac{1}{2R} E\left\{\mathbf{X}(n)\mathbf{H}\mathbf{H}^H\mathbf{X}^H(n)\right\} \tag{31}$$

$$\mathbf{R}_x = \frac{1}{\text{SF}} E\left\{\mathbf{X}(n)\mathbf{X}^H(n)\right\}. \tag{32}$$

In a real implementation, they have to be estimated using time averages instead of ensemble ones.

5 Subspace approach

The expression of $\mathbf{R}_{in}$ for both implicit and explicit redundancy situations, (23) and (31) respectively, can be easily interpreted from a subspace point of view [25,8]. Temporally, the signal of interest is contained in the signal subspace, S, and the rest of the interfering signals and thermal noise are contained both in the signal subspace, S, and in its orthogonal subspace, $S^{\perp}$; therefore, the received signal will be contained in $S \oplus S^{\perp}$ (see Figure 4). The subspace approach consists of computing $\mathbf{R}_{in}$ by using the signal component in $S^{\perp}$, i.e., the projection of the received signal on the temporal subspace orthogonal to the desired signal. Note that the calculation of $\mathbf{R}_d$ using the projection on the desired temporal signal subspace would be a worse approach, because it could contain interference leakage (see Figure 4).

For the implicit redundancy case, we can write the received model as:

$$\mathbf{X}(n) = s_d(n)\mathbf{a}_d\mathbf{c}_d^H(n) + \mathbf{N}(n) \tag{33}$$

and project its row space—temporal dimension—on the subspace orthogonal to $\mathbf{c}_d(n)$:

$$\mathbf{X}^{\perp}(n) = \mathbf{X}(n)\mathbf{P}_{c_d}^{\perp}(n) = \mathbf{N}(n)\mathbf{P}_{c_d}^{\perp}(n) \tag{34}$$

where $\mathbf{P}_{c_d}^{\perp}(n) \in \mathbb{C}^{\text{SF}\times\text{SF}}$ is the time-varying projection matrix, and $\mathbf{X}^{\perp}(n)$ the noise contained in $S^{\perp}$. The same result would be obtained using the despread block snapshot, $\tilde{\mathbf{X}}(n)$, and the fixed projection matrix $\mathbf{P}_1^{\perp}$. Hence, the expression for $\mathbf{R}_{in}$ is:

$$\begin{aligned}\mathbf{R}_{in} \triangleq \mathbf{R}_n^{\perp} &= \frac{1}{\text{SF-1}} E\left\{\mathbf{X}^{\perp}(n)\mathbf{X}^{\perp H}(n)\right\} \\ &= \frac{1}{\text{SF-1}} E\left\{\mathbf{N}(n)\mathbf{P}_{c_d}^{\perp}(n)\mathbf{N}^H(n)\right\}\end{aligned} \tag{35}$$

where the factor $(\text{SF} - 1)$ accounts for the loss of one dimension due to the temporal projection (see Appendix for further details).

Regarding the explicit redundancy case, the signal model is:

$$\mathbf{X}(n) = s_d(n)\mathbf{a}_d\mathbf{c}_d^H(n)\mathbf{G}^H + \mathbf{N}(n). \tag{36}$$

In this case, although the subspace orthogonal to $\tilde{\mathbf{c}}(n) = \mathbf{Gc}(n)$ is, in principle, time-varying, there is a subset of this subspace that remains fixed over the time, the subspace orthogonal to $\mathbf{G}$:

$$\mathbf{R}_{in} \triangleq \mathbf{R}_n^{\perp} = \frac{1}{R}E\left\{\mathbf{X}(n)\mathbf{P}_G^{\perp}\mathbf{X}(n)\right\} \tag{37}$$

where $\mathbf{P}_G^{\perp} = \mathbf{HDH}^H$ (with rank R), with $\mathbf{D}$ a diagonal matrix to normalize the columns of $\mathbf{H}$.

Regarding the definition $\mathbf{R}_{in} \triangleq \mathbf{R}_n^{\perp}$, it simply means that we are considering that the spatial structure of the interfering signals can be estimated using only the temporal component orthogonal to the temporal desired signal subspace (see Appendix for an analysis of the goodness of this assumption).

6 Design of explicit fixed time-diversity

There are two important issues in the design of the redundancy matrices, $\mathbf{G}_k$, $1 \leq k \leq K$, for a number of K users. One refers to the autocorrelation properties of the PN sequences, which have been carefully and extensively studied in the literature [26], and the other refers to the fact that these matrices have to be jointly designed so that each user redundancy structure is orthogonal to any other.

6.1 Correlation properties of the RPN sequences

Auto- and cross-correlation properties of PN sequences are very important for synchronization reasons and to provide a nearly orthogonal channelization for the users [22]. PN sequences with good correlation properties—noise-like properties—have been widely analyzed in the literature. There are a few families of such sequences that present these desirable properties, namely, maximal-length codes, Gold codes, large and small set of Kasami sequences, Hadamard sequences [26].

Due to the aforementioned reasons, if we are to modify these carefully designed PN sequences, we have to make sure not to ruin them. In the following discussion, the original time-varying spreading code—consecutive segments of the original PN sequence—is considered to be a binary *i.i.d.* sequence, i.e.,

$$E\left\{\mathbf{c}(n_1)\mathbf{c}^H(n_2)\right\} = \mathbf{I}\cdot\delta(n_1 - n_2). \tag{38}$$

Therefore, the autocorrelation function of the modified PN sequence is zero for lags greater than the spreading factor, no matter the choice of $\mathbf{G}$, because the RPN segments are linear combinations of uncorrelated PN blocks. To study smaller lags, we will use the following signal model:

$$\begin{bmatrix} \tilde{\mathbf{c}}(n) \\ \tilde{\mathbf{c}}(n-1) \end{bmatrix} = \begin{bmatrix} \mathbf{G} & \mathbf{0} \\ \mathbf{0} & \mathbf{G} \end{bmatrix} \begin{bmatrix} \mathbf{c}(n) \\ \mathbf{c}(n-1) \end{bmatrix} \tag{39}$$

where $\mathbf{c}(n) \in \mathbb{C}^{(\text{SF-R})\times 1}$ is the nth segment of the original PN sequence, and $\tilde{\mathbf{c}}(n) \in \mathbb{C}^{\text{SF}\times 1}$ is the nth segment of the redundant PN sequence. By defining the following matrices:

$$\Gamma = \begin{bmatrix} \mathbf{G} & \mathbf{0} \\ \mathbf{0} & \mathbf{G} \end{bmatrix} \tag{40}$$

$$\Gamma^{(p)} = \begin{bmatrix} \mathbf{0}_{\text{SF}\times\text{p}} & \mathbf{I}_{\text{SF}\times\text{SF}} & \mathbf{0}_{\text{SF}\times(\text{SF}-\text{p})} \end{bmatrix} \Gamma \tag{41}$$

$$\Gamma \in \mathbb{C}^{2\text{SF}\times 2(\text{SF}-R)}, \Gamma^{(p)} \in \mathbb{C}^{\text{SF}\times 2(\text{SF}-R)}$$

the RPN sequence shifted p chips can be compactly expressed as

$$\tilde{\mathbf{c}}^{(p)}(n) = \Gamma^{(p)} \begin{bmatrix} \mathbf{c}(n) \\ \mathbf{c}(n-1) \end{bmatrix}, \tag{42}$$

and the autocorrelation function is then given by

$$\begin{aligned} r(p-l) &= E\left\{\tilde{\mathbf{c}}^{(p)H}(n)\tilde{\mathbf{c}}^{(l)}(n)\right\} = \text{tr}\left\{\Gamma^{(l)}\Gamma^{(p)H}\right\} \\ &= \text{tr}\left\{ \begin{bmatrix} \overset{\leftrightarrow l}{\mathbf{0}} & \mathbf{I} & \mathbf{0} \end{bmatrix} \begin{bmatrix} \mathbf{G}\mathbf{G}^H & \mathbf{0} \\ \mathbf{0} & \mathbf{G}\mathbf{G}^H \end{bmatrix} \begin{bmatrix} \mathbf{0}\updownarrow p \\ \mathbf{I} \\ \mathbf{0} \end{bmatrix} \right\} = \text{SF}\cdot\delta_{pl} \end{aligned} \tag{43}$$

where tr$(\cdot)$ stands for the trace operator. This imposed condition simply means that each diagonal of the matrix $\mathbf{G}\mathbf{G}^H$ have to add up to zero, except the main one that must sum up the value SF. If this design criterion is not met, deterministic peaks appear in the autocorrelation function (see Figure 5(e)-(f)).

Regarding the cross-correlation properties, since the original PN sequences are uncorrelated:

$$E\left\{\mathbf{c}_i(n_1)\mathbf{c}_j^H(n_2)\right\} = \mathbf{0} \quad \text{for} \qquad i \neq j \tag{44}$$

so will be the redundant ones:

$$E\left\{\tilde{\mathbf{c}}_i^{(p)}\tilde{\mathbf{c}}_j^{(l)H}\right\} = \mathbf{0} \quad \text{for} \qquad i \neq j\,. \tag{45}$$

6.2 Joint design of the redundancy structures for multiple users

First, a simple scenario with all the users synchronized is assumed for simplicity of presentation, having the following received signal model:

$$\mathbf{X}(n) = s_d(n)\mathbf{a}_d\mathbf{c}_d^H(n)\mathbf{G}_d^H + \sum_{i=1}^{N_I} s_i(n)\mathbf{a}_i\mathbf{c}_i^H(n)\mathbf{G}_i^H + \mathbf{W}(n). \tag{46}$$

from which we can either estimate $\mathbf{R}_d$ or $\mathbf{R}_{in}$. The estimation of $\mathbf{R}_d$ is (aside from a scalar factor)

$$\begin{aligned}
\hat{\mathbf{R}}_d &= E\left\{\mathbf{X}_1\mathbf{X}_2^H + \mathbf{X}_2\mathbf{X}_1^H\right\} = E\left\{\mathbf{X}\left(\mathbf{H}_1\mathbf{H}_2^H + \mathbf{H}_2\mathbf{H}_1^H\right)\mathbf{X}^H\right\} \\
&= p_d\mathbf{a}_d E\left\{\mathbf{c}_d^H\mathbf{G}_d^H\mathbf{R}_{H_{1221}}\mathbf{G}_d\mathbf{c}_d\right\}\mathbf{a}_d^H \\
&\quad + \sum_{i=1}^{N_I} p_i\mathbf{a}_i E\left\{\mathbf{c}_i^H\mathbf{G}_i^H\mathbf{R}_{H_{1221}}\mathbf{G}_i\mathbf{c}_i\right\}\mathbf{a}_i^H + E\left\{\mathbf{W}\mathbf{R}_{\mathbf{H_{1221}}}\mathbf{W}^H\right\} \\
&= \operatorname{tr}\left\{\mathbf{G}_d^H\mathbf{R}_{H_{1221}}\mathbf{G}_d\right\} p_d\mathbf{a}_d\mathbf{a}_d^H + \sum_{i=1}^{N_I}\operatorname{tr}\left\{\mathbf{G}_i^H\mathbf{R}_{H_{1221}}\mathbf{G}_i\right\} p_i\mathbf{a}_i\mathbf{a}_i^H
\end{aligned} \tag{47}$$

where the definition $\mathbf{R}_{H_{1221}} \triangleq \mathbf{H}_1\mathbf{H}_2^H + \mathbf{H}_2\mathbf{H}_1^H$ has been used, and it has been assumed that the thermal noise from different branches is uncorrelated, i.e., $E\left\{\mathbf{W}_1\mathbf{W}_2^H\right\} = \mathbf{0}$. To have a proper estimation of $\mathbf{R}_d$, the following condition has to be verified:

$$\operatorname{tr}\left\{\mathbf{G}_i^H\mathbf{R}_{H_{1221}}\mathbf{G}_i\right\} = 0 \quad \text{for} \quad 1 \leq i \leq N_I \tag{48}$$

where $\mathbf{G}_i^H\mathbf{R}_{H_{1221}}\mathbf{G}_i = \mathbf{0}$ would be a sufficient condition but not necessary.

Exactly the same design criterion can be derived from imposing a correct estimation of $\mathbf{R}_{in}$, which is (aside from a scalar factor)

$$\begin{aligned}
\hat{\mathbf{R}}_{in} &= E\left\{(\mathbf{X}_1(n) - \mathbf{X}_2(n))\,(\mathbf{X}_1(n) - \mathbf{X}_2(n))^H\right\} \\
&= E\left\{\mathbf{N}_1(n)\mathbf{N}_1^H(n)\right\} + E\left\{\mathbf{N}_2(n)\mathbf{N}_2^H(n)\right\} \\
&\quad - E\left\{\mathbf{N}_1(n)\mathbf{N}_2^H(n)\right\} - E\left\{\mathbf{N}_2(n)\mathbf{N}_1^H(n)\right\}.
\end{aligned} \tag{49}$$

For the previous estimation to have as much interfering power as possible, $E\left\{\mathbf{N}_1(n)\mathbf{N}_2^H(n)\right\}$ has to be as low as possible, which coincides with the previous condition. In this case, we can also write $\hat{\mathbf{R}}_{in}$ as:

$$\begin{aligned}\hat{\mathbf{R}}_{in} &= \frac{1}{R}E\left\{\mathbf{X}(n)\mathbf{P}_{G_d}^{\perp}\mathbf{X}(n)\right\}\\ &= \frac{1}{R}\sum_{i=1}^{N_i} p_i\mathbf{a}_i E\left\{\mathbf{c}_i^H\mathbf{G}_i^H\mathbf{P}_{G_d}^{\perp}\mathbf{G}_i\mathbf{c}_i\right\}\mathbf{a}_i^H + \frac{1}{R}E\left\{\mathbf{W}\mathbf{P}_{\mathbf{G_d}}^{\perp}\mathbf{W}^H\right\}\end{aligned} \tag{50}$$

from which, imposing a proper estimation, we have:

$$\mathrm{tr}\left\{\mathbf{G}_i^H\mathbf{P}_{G_d}^{\perp}\mathbf{G}_i\right\} = \left\|\mathbf{P}_{G_d}^{\perp}\mathbf{G}_i\right\|_F^2 = \mathrm{R} \tag{51}$$

where $\|\cdot\|_F$ denotes Frobenius norm. Note that both conditions are completely equivalent. The last one, however, clearly states that the design of the **G**'s can be done independently to that of the **H**'s.

For the unsynchronized case, a more general signal model has to be used:

$$\tilde{\mathbf{c}}^{(p)}(n) = \Gamma^{(p)}\begin{bmatrix}\mathbf{c}(n)\\ \mathbf{c}(n-1)\end{bmatrix} \tag{52}$$

where $\Gamma^{(p)}$ is defined as in (41), so that the received signal can be expressed as:

$$\begin{aligned}\mathbf{X}(n) &= s_d(n)\mathbf{a}_d\mathbf{c}_d^H(n)\mathbf{G}_d^H\\ &\quad + \sum_{i=1}^{N_I}\mathbf{a}_i\left[\, s_i(n)\mathbf{c}_i^H(n)\;\; s_i(n-1)\mathbf{c}_i^H(n-1)\,\right]\Gamma_i^{(p_i)H} + \mathbf{W}(n)\end{aligned} \tag{53}$$

and the design criterion is:

$$\left\|\mathbf{P}_{G_d}^{\perp}\Gamma_i^{(p)}\right\|_F^2 = \mathrm{R} \qquad \text{for} \quad 1 \le i \le N_I, \quad 0 \le p < \mathrm{SF} \ . \tag{54}$$

Therefore, the design of **G** is subject to two conditions, expressed by equations (43) and (54). This implies that extensive search methods have to be employed to find the redundancy matrix for each user. For this reason, small values of R are easier to handle.

Regarding the design of **H**, it is straightforward to derive from its corresponding **G** by performing the single value decomposition on **G**:

$$\mathbf{G} = \mathbf{U}\mathbf{D}\mathbf{V}^H = \begin{bmatrix}\mathbf{U}_1 & \mathbf{U}_2\end{bmatrix}\begin{bmatrix}\mathbf{D}_1\\ \mathbf{0}\end{bmatrix}\mathbf{V}^H = \mathbf{U}_1\mathbf{D}_1\mathbf{V}^H \tag{55}$$

where $\mathbf{U}_2$ spans the null space and is orthogonal to the range space $\mathbf{U}_1^H\mathbf{U}_2 = \mathbf{0}$. Therefore, the matrix $\mathbf{H}$ can be easily defined as $\mathbf{H} = \mathbf{U}_2$, so that $\mathbf{G}^H\mathbf{H} = \mathbf{0}$. Note that $\mathbf{P}_G^{\perp} = \mathbf{U}_2\mathbf{U}_2^H$. In addition, from a visual inspection of the structure of $\mathbf{G}$, it is simple to define $\mathbf{H}_1$ and $\mathbf{H}_2$ as can be seen from Figure 3.

7 Practical issues

In a practical situation, the estimation of $\mathbf{R}_{in}$ is far better than the estimation of $\mathbf{R}_d$. The reason is that in the latter there may be some leakage of undesired signals, whereas in the former no desired signal will ever be present—the worst thing that can happen is that some components of the interfering signals lay on the desired signal subspace and, therefore, those interfering signals appear in $\mathbf{R}_{in}$ with less power (see Figure 4).

Once the covariance matrices associated to a desired user are available, we can use them to perform maximum SINR beamforming in a single-user fashion. Since the rest of the users do not verify the self-prediction property of the selected user, they will be nulled out (or at least attenuated according to the maximum SINR criterion). Nevertheless, the idea of self-reference could be extended to a more general case by allowing a subset of users to survive after beamforming. However, this is out of the scope of the present paper.

For frequency-selective scenarios, the same algorithm can be directly applied on a finger basis reminiscent of the RAKE receiver [14]. The beamformer corresponding to a particular finger with a specific delay will null out (or attenuate) all signals that do not verify the cross-correlation properties for that particular delay, i.e., signals from other users or multi-access interference (MAI) and also the inter-symbol interference (ISI) of the desired user.

It is important to remark that once the beamvectors are designed according to any criterion, they have to be used on a chip basis. After applying the beamvectors on the block snapshot defined in (18) or (46), a chip sequence with no spatial dimension is obtained ready for a conventional matched filtering or despreading stage. In principle, designing the beamvectors to maximize the SINR or, equivalently, to minimize the mean square error (MSE) on a chip level, unlike doing it on a symbol level, does not necessarily have to be optimum. However, as was shown in [27], when binary *i.i.d.* spreading codes are used, both criteria coincide. The same cannot be said for the case of fixed or deterministic codes, not treated in this paper (see [24] for a blind subspace-based method for the case of deterministic codes).

It is worth noting that, unlike in most subspace-based methods, no singular value decomposition (SVD) or eigenvalue decomposition (EVD) are required for the estimation of the covariance matrices. This represents a significant reduction on the computational burden and is considered a key feature of the proposed methods.

8 Simulations

In order to evaluate and compare the beamforming methods based on the implicit (PN) and explicit (RPN) redundancy, Monte-Carlo simulations were performed with a uniform linear array of 7 sensors, with a half-wavelength separation, in a hostile scenario to test the robustness of the algorithms. The carrier frequency was $f_c = 900$MHz, and the chip rate $R_c = 4.096$MHz ($T_c = 244.14$ns). A simple and suboptimum single-user detector consisting of a matched filter was used after the beamforming stage. The scenario was composed of a BPSK signal of interest with a DOA of 15^o(with different values of E_b/N_0), and 4 interfering BPSK signals—other users—impinging from angles of 0, -30, 50, and 80 degrees (with E_b/N_0 of 30dB, 20dB, 40dB, and 20dB) respectively, yielding a total I_0/N_0=25.6dB, with I_0 the global chip-level interference power per sensor. Gold sequences of length 1023 and SF=31 were utilized (for the RPN the simple case of R=2 was used). To model the angular spread of the steering vectors, a Laplacian Power Angular Spectrum with a power azimuth spread (AS) of 8 degrees—corresponding to an outdoor or outdoor-to-indoor scenario—was used according to [28]. The temporal dispersion of the channel was generated with a Pedestrian model type A as specified by ETSI [29], which exhibits a low temporal dispersion (a r.m.s. delay spread of 45ns) compared to T_c, with a speed of 3 km/h.

In Figure 6, the bit error rate (BER) of the proposed methods can be seen compared to that of a classical TRB (with 10% of the bits as a training sequence) aided with a decision-directed (DD) approach, and to the minimum BER theoretically achievable—for the array and the single sensor case. From the simulations results, it can be seen how the proposed diversity methods perform slightly better than the TRB+DD (with 10% training sequence) even though they do not use any side information. The PN approach clearly outperforms the RPN one, because it uses an orthogonal subspace of dimension (SF-1)=30, whereas the RPN just uses an orthogonal subspace of dimension R=2.

In Figure 7, the ensemble SINR evolution of an adaptive scheme (using the power iteration approach) of all the approaches during 160 symbols is depicted (updating the estimated matrices at each new received symbol). Again, the convergence speed of the RPN approach is slower than that of the PN or TRB. The SINR is given at a chip level, i.e., before the despreading stage, which theoretically would give a gain of $10\log_{10}$SF$\simeq$ 15 dB.

In Figure 8, we show the beamformer, after convergence, for the RPN-based method compared to the optimum one. It can be seen how well the interfering signals are nulled out, whereas the main beam is steered towards the desired signal. In this case, the users were modeled as point-source signals (AS=0) to allow a proper visual beamformer inspection (see Figure 8).

9 Conclusions

In this paper, after a general introduction of the concepts of diversity and exact prediction property, two self-reference beamforming approaches for DS-CDMA have been derived based on the redundancy temporal structure of the DS-CDMA signals. Depending on whether the implicit redundancy of a regular PN sequence is used, or an explicit redundancy is intentionally introduced in the PN in transmission, two approaches arise (in fact, the former is a particular case of the latter). Those approaches, unlike most blind subspace-based methods, do not require SVD nor EVD, with a great reduction of the complexity of the algorithms and the consequent decrease of the computational load.

For the case of redundancy explicitly introduced, we have derived the conditions to be met by the redundancy structures so that the global performance of the DS-CDMA system is not degraded (PN correlation properties and separability of users in multiuser scenarios). This particular method does not require PN synchronization to start working, therefore, the spatial processing can help the synchronization stage.

The blind self-reference beamforming approaches described in the present paper, despite the lack of side information, have been shown via Monte-Carlo simulations to outperform the classical TRB (using 10% of the bits as a training sequence) on low dispersive channels, which is a very interesting result to take into account before designing a time reference based DS-CDMA communication system.

10 Acknowledgment

The authors wish to thank the anonymous reviewers for their helpful comments on the manuscript.

Appendix

A Spatial structure of a temporally projected signal

Expressing the noise block snapshot as

$$\mathbf{N} = \left[\mathbf{n}_1 \cdots \mathbf{n}_{\mathrm{SF}} \right], \tag{A.1}$$

and assuming temporally uncorrelated (white) noise and a stationary spatial structure:

$$E\left\{ \mathbf{n}_i \mathbf{n}_j^H \right\} = \mathbf{R}_n \delta_{ij}, \tag{A.2}$$

the noise covariance matrix is

$$E\left\{ \mathbf{N}\mathbf{N}^H \right\} = \mathrm{SF} \cdot \mathbf{R}_n. \tag{A.3}$$

Note that the dimension of the row-space of $\mathbf{N}$ is SF.

Using the Cholesky decomposition $\mathbf{R}_n = \mathbf{L}\mathbf{L}^H$, a spatially whitened version of the noise can be obtained as follows:

$$\tilde{\mathbf{n}}_i = \mathbf{L}^{-1}\mathbf{n}_i \tag{A.4}$$

so that

$$E\left\{ \tilde{\mathbf{n}}_i \tilde{\mathbf{n}}_j^H \right\} = \delta_{ij} \cdot \mathbf{I}. \tag{A.5}$$

If we perform a rotation on $\tilde{\mathbf{N}}$, we obtain $\mathbf{M} = \tilde{\mathbf{N}}\mathbf{U}$, where $\mathbf{U}\mathbf{U}^H = \mathbf{U}^H\mathbf{U} = \mathbf{I}$, and the statistics remain unaffected:

$$E\left\{ \mathbf{m}_i \mathbf{m}_j^H \right\} = \delta_{ij} \cdot \mathbf{I}, \quad \text{and} \tag{A.6}$$

$$E\left\{ \mathbf{M}\mathbf{M}^H \right\} = \mathrm{SF} \cdot \mathbf{I} \tag{A.7}$$

A projection of the row-space—temporal domain—is performed using $\mathbf{P} = \mathbf{U}\mathbf{D}\mathbf{U}^H$, where $\mathbf{D} \in \mathbb{C}^{\mathrm{SF}\times\mathrm{SF}}$ is a diagonal matrix containing N_1 ones and N_0 zeros, yielding

$$\tilde{\mathbf{N}}^{\perp} = \tilde{\mathbf{N}}\mathbf{P} = \mathbf{M}\mathbf{D}\mathbf{U}^H = \mathbf{M}_1\mathbf{U}_1^H, \tag{A.8}$$

where $\mathbf{U}_1 \in \mathbb{C}^{\mathrm{SF}\times\mathrm{N}_1}$ contains the columns of $\mathbf{U}$ corresponding to the non-zero eigenvalues, i.e., we can perform the following decompositions

$$\mathbf{U} = \left[\mathbf{U}_1 \; \mathbf{U}_2 \right], \quad \text{and} \tag{A.9}$$

$$\mathbf{M} = \left[\mathbf{M}_1 \; \mathbf{M}_2 \right]. \tag{A.10}$$

As a consequence,

$$E\left\{\tilde{\mathbf{N}}^{\perp}\tilde{\mathbf{N}}^{\perp H}\right\} = E\left\{\mathbf{M}_1\mathbf{M}_1^H\right\} = \mathrm{N}_1 \cdot \mathbf{I}. \qquad \text{(A.11)}$$

Therefore it has been proved that

$$E\left\{\mathbf{NPN}^H\right\} = \mathbf{L}E\left\{\tilde{\mathbf{N}}\mathbf{P}\tilde{\mathbf{N}}^H\right\}\mathbf{L}^H = \mathrm{N}_1 \cdot \mathbf{R}_n, \qquad \text{(A.12)}$$

which clearly shows that the noise spatial structure can be estimated using the noise component contained in the temporal subspace orthogonal to the desired signal.

References

[1] J. R. Treichler, M. G. Larimore, New processing techniques based on the constant modulus adaptive algorithm, IEEE Trans. on Acoustics, Speech and Signal Processing ASSP-33 (2) (1985) 420–431.

[2] R. Gooch, J. Lundell, The CM array: an adaptive beamformer for constant modulus signals, Proc. IEEE ICASSP'86 (1986) 2523–2526.

[3] A. L. Swindlehurst, S. Daas, J. Yang, Analysis of a decision directed beamformer, IEEE Trans. on Signal Processing 43 (12) (1995) 2920–2927.

[4] L. D. Lathauwer, B. D. Moor, J. Vandewalle, Independent component analysis based on higher-order statistics only, Proc. IEEE Signal Processing Workshop on Statistical Signal Array Processing (1996) 356–359.

[5] E. Gönen, J. M. Mendel, Applications of cumulants to array processing-part III: Blind beamforming for coherent signals, IEEE Trans. on Signal Processing 45 (1997) 2252–2264.

[6] B. G. Agee, S. V. Schell, W. A. Gardner, Spectral self-coherence restoral: A new approach to blind adaptive signal extraction using antenna arrays, Proceedings of the IEEE 78 (4) (1990) 753–767.

[7] D. P. Palomar, M. Nájar, M. A. Lagunas, Self-reference spatial diversity processing for spread spectrum communications, AEÜ International Journal of Electronics and Communications 54 (5) (2000) 267–276.

[8] M. K. Tsatsanis, G. B. Giannakis, Transmitter induced cyclostationarity for blind channel equalization, IEEE Trans. on Signal Processing 45 (7) (1997) 1785–1794.

[9] G. Vázquez, F. Rey, M. Lamarca, Redundancy in block coded modulations for channel equalization based on spatial and temporal diversity, in: Proc. of the IEEE-ICASSP'99, Phoenix, AZ, 1999, pp. 2711–2714.

[10] M. A. Lagunas, A. I. Pérez-Neira, M. G. Amin, J. Vidal, Spatial processing for frequency diversity schemes, IEEE Trans. on Signal Processing 48 (2) (2000) 353–362.

[11] D. P. Palomar, M. A. Lagunas, Optimum self-reference spatial diversity processing for FDSS and FH communication systems, in: Proc. EUSIPCO-2000, Vol. III, Tampere (Finland), 2000.

[12] D. P. Palomar, M. A. Lagunas, Self-reference beamforming for DS-CDMA communication systems, in: Proc. IEEE ICASSP-2000, Vol. V, Istanbul, Turkey, 2000, pp. 3001–3004.

[13] D. P. Palomar, M. A. Lagunas, Blind beamforming for DS-CDMA systems, in: Proc. Fifth Bayona Workshop on Emerging Technologies in Telecomm., Bayona, Vigo (Spain), 1999, pp. 83–87.

[14] J. G. Proakis, Digital Communications, 3rd Edition, McGraw-Hill, New York, 1995.

[15] G. K. Kaleh, Frequency-diversity spread-spectrum communication system to counter bandlimited gaussian interference, IEEE Trans. on Comm. 44 (7) (1996) 886–893.

[16] V. Weerackody, Diversity for the direct-sequence spread spectrum system using multiple transmit antennas, in: Proc. ICC'93, Vol. 3, Geneva, Switzerland, 1993, pp. 1775–1779.

[17] R. Vaughan, Polarization diversity in mobile communications, IEEE Trans. on Vehicular Technology 39 (3) (1990) 177–186.

[18] A. Sayeed, B. Aazhang, Joint multipath-Doppler diversity in mobile wireless communications, IEEE Trans. on Communications 47 (1) (1999) 123–132.

[19] S. Haykin, Adaptive Filter Theory, 3rd Edition, Prentice Hall, New Jersey, 1996.

[20] M. Nájar, X. Mestre, M. A. Lagunas, Two-stage code reference beamformer for the reception of frequency hopping modulated signals, Signal Processing (EURASIP) 80 (12) (2000) 2623–2632.

[21] G. H. Golub, C. F. V. Loan, Matrix Computations, The Johns Hopkins University Press, Baltimore, MD, 1996.

[22] R. L. Peterson, R. E. Ziemer, D. E. Borth, Introduction to Spread Spectrum Communications, Prentice Hall, 1995.

[23] B. Suard, A. F. Naguib, G. Xu, A. Paulraj, Performance of CDMA mobile communication systems using antenna arrays, in: Proceeding of the IEEE ICASSP-93, Minneapolis, 1993, pp. IV153–IV156.

[24] D. Gesbert, J. Sorelius, A. Paulraj, Blind multi-user MMSE detection of CDMA signals, in: Proc. of the IEEE ICASSP'98, Seatle, WA, 1998, pp. 3161–3164.

[25] E. Moulines, P. Dehamel, J.-F. Cardoso, S. Mayrargue, Subspace methods for the blind identification of multichannel FIR filters, IEEE Trans. on Signal Processing 43 (2) (1995) 516–525.

[26] D. V. Sarware, M. B. Pursley, Crosscorrelation properties of pseudorandom and related sequences, Proceedings of the IEEE 68 (5) (1980) 593–619.

[27] H. Liu, M. D. Zoltowski, Blind equalization in antenna array CDMA systems, IEEE Trans. on Signal Processing 45 (1) (1997) 161–172.

[28] K. I. Pedersen, P. E. Mogensen, B. H. Fleury, A stochastic model of the temporal and azimuthal dispersion seen at the base station in outdoor propagation environments, IEEE Trans. on Vehicular Technology 49 (2) (2000) 437–447.

[29] ETSI, Selection Procedures for the Choice of Radio Transmission Technologies of the UMTS (UMTS 30.03), Tech. Rep. TR101 112, v3.2.0, ETSI .

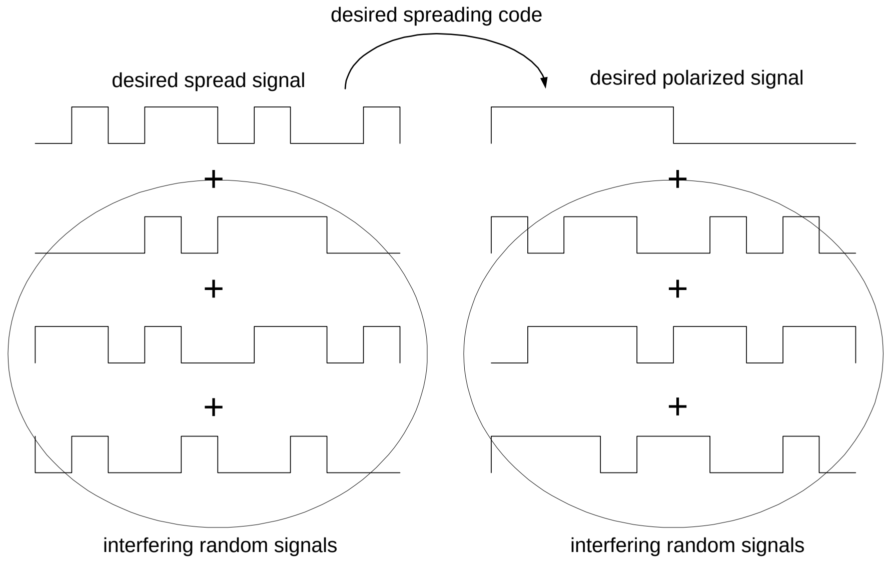

Fig. 1. Illustration of the despreading/polarization process using the spreading code of the user of interest. The desired signal becomes fully correlated, whereas the interfering ones remain random and uncorrelated.

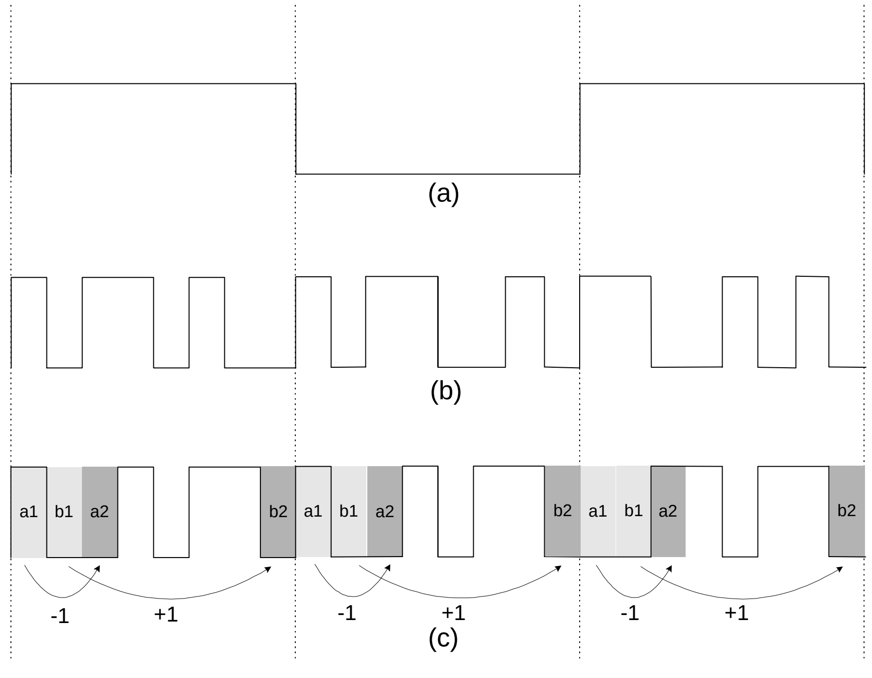

Fig. 2. Example of Time Diversity in DS-CDMA: (a) original bit sequence, (b) spread bit sequence using a standard PN, and (c) spread bit sequence using a fixed redundancy structure (redundant PN).

$$\mathbf{G} = \begin{bmatrix} 1 & 0 & 0 & 0 & 0 & 0 \\ 0 & 1 & 0 & 0 & 0 & 0 \\ -1 & 0 & 0 & 0 & 0 & 0 \\ 0 & 0 & 1 & 0 & 0 & 0 \\ 0 & 0 & 0 & 1 & 0 & 0 \\ 0 & 0 & 0 & 0 & 1 & 0 \\ 0 & 0 & 0 & 0 & 0 & 1 \\ 0 & 1 & 0 & 0 & 0 & 0 \end{bmatrix} \quad \mathbf{H}_1^{\mathbf{T}} = \begin{bmatrix} 1 & 0 & 0 & 0 & 0 & 0 & 0 & 0 \\ 0 & 1 & 0 & 0 & 0 & 0 & 0 & 0 \end{bmatrix} \quad \mathbf{H}_2^{\mathbf{T}} = \begin{bmatrix} 0 & 0 & -1 & 0 & 0 & 0 & 0 & 0 \\ 0 & 0 & 0 & 0 & 0 & 0 & 0 & 1 \end{bmatrix}$$

$$\mathbf{G}^{\mathbf{H}}\mathbf{H} = \mathbf{0}$$

Fig. 3. Example of a redundancy matrix $\mathbf{G}$ and a check-parity matrix $\mathbf{H} = \mathbf{H}_1 - \mathbf{H}_2$.

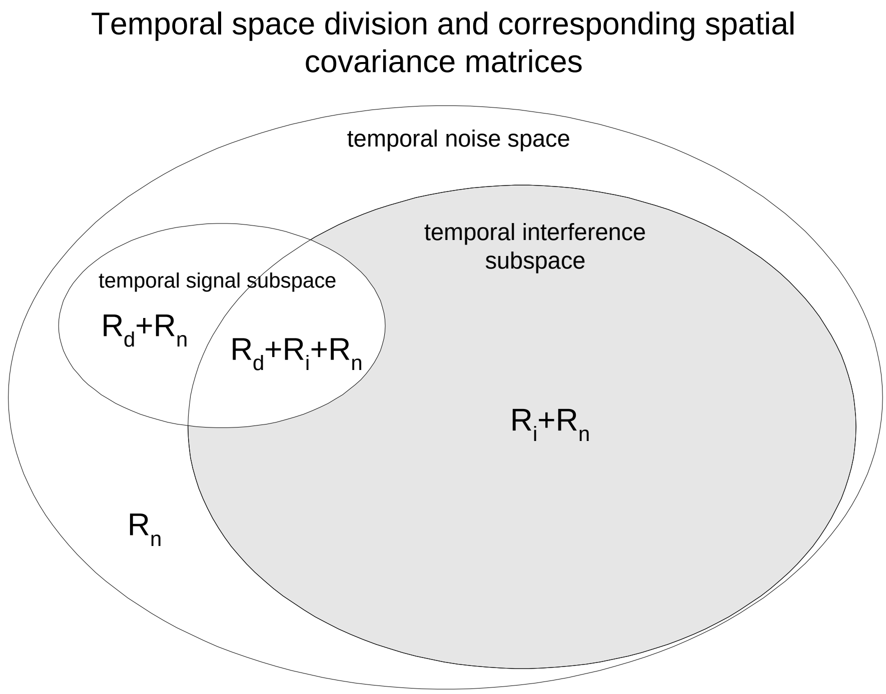

Fig. 4. Scheme of the subspaces in the temporal domain and their corresponding spatial covariance matrices.

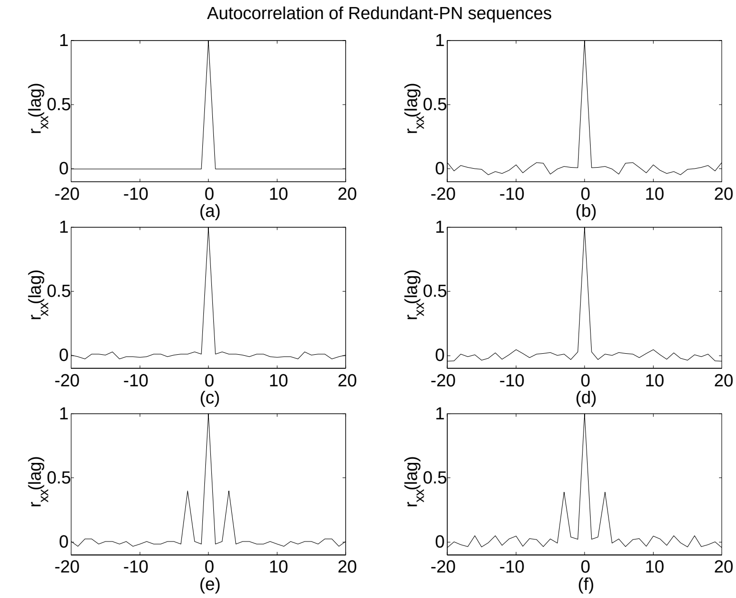

Fig. 5. Autocorrelation of different PN sequences: (a) original maximal seq., (b) original random seq., (c) redundant maximal seq., (d) redundant random seq., (e) redundant maximal seq. wrongly designed, and (f) redundant random seq. wrongly designed.

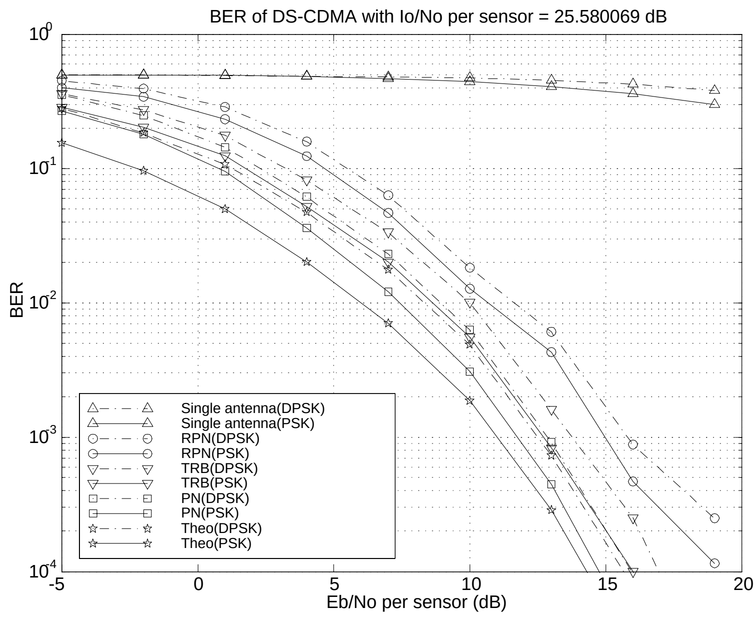

Fig. 6. Uncoded BER of the different methods (TRB+DD using 10% as training sequence, PN-based, RPN-based) along with the theoretically minimum achievable BER for BPSK and binary DPSK. The scenario was composed of a desired signal with DOA of 15^o and 4 interfering signals with DOA's of 0^o, -30^o, 50^o and 80^o (E_b/N_o of 30dB, 20dB, 40dB and 20dB) respectively. Gold sequences of length 1023 and SF=31 were used.

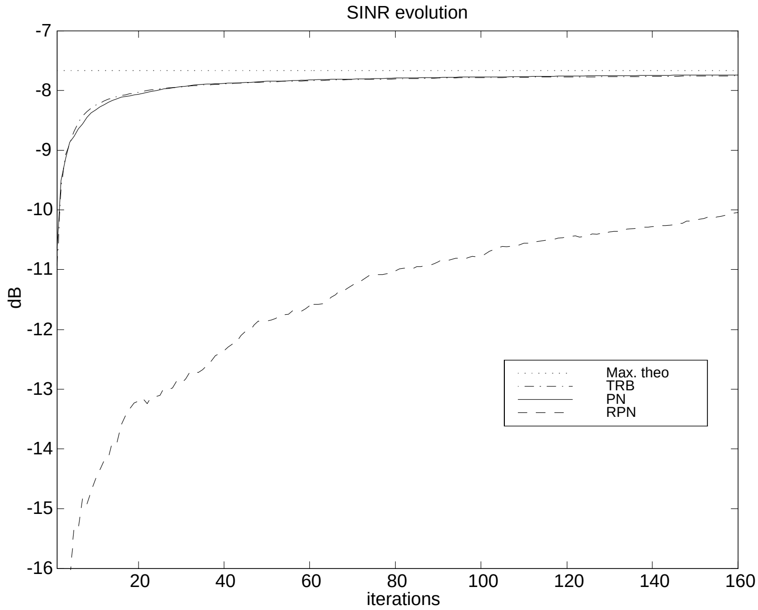

Fig. 7. Ensemble average of the SINR evolution during 160 symbols for an array of 7 elements.

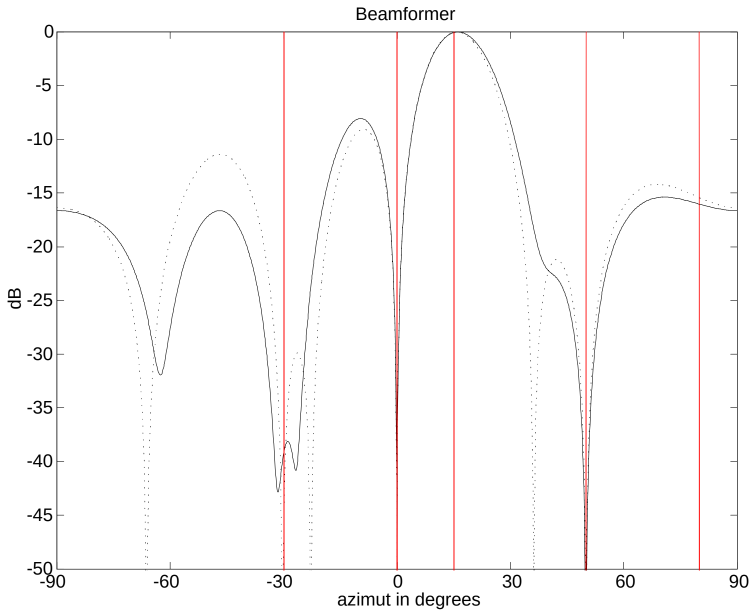

Fig. 8. Beamforming of the RPN-based approach—solid line—after convergence compared to the optimum one—dotted line. Scenario composed of a signal of interest with $E_b/N_0 = 5$dB (15^o) and 4 interfering signals impinging from angles of 0, -30, 50, and 80 degrees (with E_b/N_0 of 30dB, 20dB, 40dN, and 20dB). A flat-frequency channel was utilized with a zero speed. The users were modelled as point-source signals (AS=0).